

SOME SURFACTANTS AS CORROSION INHIBITORS FOR C-STEEL IN ACIDIC SOLUTIONS

Y.A. Elewady, A.S. Fouda and H.K. Abd El-Aziz

Chemistry Department, Faculty of Science, El-Mansoura University, El Mansoura-35516, Egypt E-mail: yehiaelewady@yahoo.com

Received : (16/5/2010)

ABSTRACT

The corrosion inhibition effect of three different types of surfactant, namely, dodecyl trimethyl ammonium chloride (DTAC), octyl phenol poly(ethylene glycol ether)_x (TX-100) and dioctyl sodium sulfosuccinate (AOT) have been used as corrosion inhibitors for 1037 C-steel in 0.5 M HCl. The inhibition properties of the inhibitors were studied by means of weight loss, potentiodynamic polarization and electrochemical impedance spectroscopy (EIS) measurements. The results show that the order of inhibition efficiency is DTAC > TX-100 > AOT. Polarization curves indicate that investigated surfactants are mixed-type inhibitors, affecting both cathodic and anodic corrosion processes. Adsorption of these surfactants on C-steel surface was found to obey Langmuir's isotherm. The calculated free energies from Langmuir adsorption isotherm indicate that the investigated surfactants adsorb on C-steel by mixed mode of adsorption (physisorption and chemisorption) in 0.5 M HCl. The results obtained from the different techniques are in good agreement.

Keywords: C-steel; HCl; corrosion inhibition; surfactants; EIS; EFM

INTRODUCTION

In oil fields HCl solution is recommended as the cheapest way to dissolve calcium carbonate, CaCO₃, scale inside the pipelines under most conditions. Accordingly, corrosion inhibitors must be injected with the HCl solution to avoid the destructive effect of acid on the surface of the pipe lines [Oddo *et al.*, (1982)]. C-steel has been widely employed as a construction materials for pipe work in the oil and gas production such as down hole tubular, flow lines and transmission pipelines [Ridd *et al.*, (1989)]. Surfactants are compounds that can be found in a multitude of domains, from industrial settings to research laboratories and are the part of our daily lives. Mixture of surfactants have found many application in technology. These mixtures often show synergetic effects, which are evidence of non ideal behavior and are the reason of their extensive use in industry. The surfactants inhibitor has many advantages such as high inhibition efficiency, low price, low toxicity and easy production [Banerjee *et al.*, (1992)]. An increase in inhibitory action was observed when the concentration of the surfactant in the corrosive solution approaches the critical micelle concentration (CMC). Above this value, there was no further increase in the efficiency that remains constant

for further increase in surfactant concentration. In the absence of a charged head group, the driving force of micellization is the hydrophobic force and Van der Waals attractions. The strong interaction between water molecules repels the hydrocarbon chain from the water bulk phase. This drives the surfactants to form aggregates where the hydrophilic head groups conceal the hydrocarbon chains. It has been observed that the adsorption of these inhibitors depends on the physico-chemical properties of the functional groups and the electron density at the donor atom. The adsorption occurs due to the interaction of the lone pair and/or π -orbitals of inhibitor with d-orbitals of the metal surface atoms, which evokes a greater adsorption of the inhibitor molecules onto the surface, leading to the formation of a corrosion protection film [Olivares *et al.*, (2006) and Popova *et al.*, (2003)]. The adsorption is also influenced by the structure and the charge of metal surface, and the type of testing electrolyte [Lagrenée *et al.*, (2002), Tamil Selvi *et al.*, (2003) and Kissi *et al.*, (2006)].

The aim of the present paper was to determine the effectiveness of the investigated surfactants as corrosion inhibitors, using the chemical and the electrochemical techniques. These data were used to determine the inhibition efficiency of these compounds.

EXPERIMENTAL

1. Chemicals and Materials

Hydrochloric acid (37%wt), ethyl alcohol and acetone was purchased from Algamhoria Co. (Egypt). Surfactants (Dodecyl Trimethyl Ammonium Chloride: DTAC ($C_{12}H_{25}N(CH_3)_3 \cdot Cl$), Octyl phenol poly(ethylene glycol ether)_x: TX-100 ($C_{34}H_{62}O_{11}$ for $x=10$) and Dioctyl sodium sulfosuccinate: AOT ($C_{20}H_{37}O_7NaS$) were obtained from Aldrich Chemical Company. The molecular structure of DTAC, TX-100 and AOT are shown in Fig. (1). Distilled water was used for preparing test solutions for all measurements. The corrosion tests were performed on 1037 carbon steel. Rectangular specimens with dimensions 2.00 cm x 2.00 cm x 0.20 cm were used for weight loss measurements. For electro-chemical tests, the exposed surface area of carbon steel was 1.00 cm².

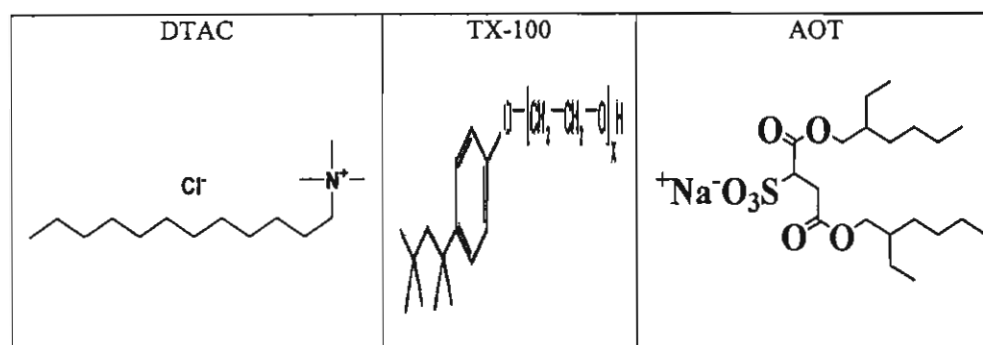


Fig. (1): Molecular structure of DTAC, TX-100 and AOT

2. METHOS

2.1. Weight loss measurements

Medium C-steel specimens were mechanically polished with 80, 220, 400, 600, 1000, 1200 grades of emery paper and degreased with acetone, rinsed with distilled water two times and finally dried between filter papers. After weighting accurately, the specimens were immersed in 100 ml of 0.5 M HCl with and without different concentrations of surfactants at 30 °C. After different immersion times (30, 60, 90, 120, 150 and 180 min), the C-steel samples were taken out, washed with distilled water, dried and weighed accurately. The experiments were done in triplicate and the average value of the weight loss was taken. The weight loss values are used to calculate the corrosion rate (CR) in millimeter per year ($\text{mm} \cdot \text{y}^{-1}$) by the relation:

$$CR = \frac{\text{Weight loss (g)} * K}{\text{Alloy Density (g / cm}^3) * \text{Exposed Area (cm}^2) * \text{Exposure Time (hr)}} \quad (1)$$

where K is the constant and equals to 8.75×10^4 , when the exposed surface area calculated by cm^2 .

The inhibition efficiency (IE %) and the degrees of surface coverage (θ) were calculated from the following equations:

$$IE \% = \frac{CR^* - CR}{CR^*} \times 100 \quad (2)$$

$$\theta = \frac{CR^* - CR}{CR^*} \quad (3)$$

where CR^* and CR are the corrosion rates of C- steel in the absence and in the presence of inhibitor ,respectively.

2.2. Electrochemical measurements

Three electrochemical techniques, namely potentiodynamic polarization, ac electrochemical impedance spectroscopy (EIS), and electrochemical frequency modulation (EFM), were used to study the corrosion behavior. All experiments were conducted in a conventional three electrodes glass cell. A Pt electrode as counter electrode and a saturated calomel electrode as reference electrode were used in this study. The C-steel specimen was machined in to rectangular (1 cm x1 cm x 0.3 cm) and sealed with epoxy resin leaving a working area of 1 cm^2 . The specimens were polished , degreased and rinsed as described before.

Potentiodynamic polarization experiments were carried out using a VoltaLab PGZ 100 system connected to personal computer with VoltaMaster 4 version 7.08 software for calculation. All the experiments were carried out at temperature ($30 \text{ }^\circ\text{C} \pm 1 \text{ }^\circ\text{C}$). Equilibrium time leading to steady state of the specimens was 20 min and the open circuits potential (OCP) was noted. The potentiodynamic curves were recorded from -900 to -200 mV at a scan rate 2 mV s^{-1} .

The calculation is performed as follows:

$$CR.(\text{mm/year}) = \frac{I_{\text{corr}} (\text{A/cm}^2) \times M (\text{g})}{D (\text{g/cm}^3) \times V} \times 3270 \quad (4)$$

with: $3270 = 10 \times [1 \text{ year (in seconds)} / 96497.8]$ and $96497.8 = 1 \text{ Faraday in Coulombs}$.
The inhibition efficiency was (IE %) calculated from:

$$IE_p \% = \frac{I_{\text{corr}}^0 - I_{\text{corr}}}{I_{\text{corr}}^0} \times 100, \quad IE_p \% = \frac{R_p^* - R_p}{R_p^*} \times 100 \quad (5)$$

where i_{corr}^0 and i_{corr} are the corrosion current densities of uninhibited and inhibited solution, respectively. R_p and R_p^* are the polarization resistance of uninhibited and inhibited solution, respectively.

Electrochemical impedance spectroscopy (EIS) and electrochemical frequency modulation (EFM) experiments were carried out using Gamry Instrument Series G 750™ Potentiostat/Galvanostat/ZRA with a Gamry framework system based on ESA400. Gamry applications include software EIS300 for EIS measurements, and EFM140 to calculate the corrosion current and the Tafel constants for EFM measurements. A computer was used for collecting data. Echem Analyst 5.5 Software was used for plotting, graphing and fitting data. EIS measurements were carried out in a frequency range of 100 kHz to 100 mHz with amplitude of 5 mV peak-to-peak using ac signals at respective corrosion potential. EFM carried out using two frequencies 0.2 and 0.5 Hz. The base frequency was 0.1 Hz. In this study, we use a perturbation signal with amplitude of 10 mV for both perturbation frequencies (0.2 and 0.5 Hz).

RESULTS AND DISSCUSION

1. Weight loss measurements

Table(1) shows the dependence of inhibition efficiency (IE %) on varying concentration of surfactants (AOT, TX-100, DTAC) in the range from $4.0 \times 10^{-5} \text{ mol l}^{-1}$ to $8.0 \times 10^{-4} \text{ mol l}^{-1}$. The data of Table (1) show that, at constant temperature the inhibition efficiency increases with increasing the concentration of the surfactant and the IE% tends to decrease in the following order: DTAC > TX-100 > AOT. The inhibition action of surfactants in HCl cannot be simply considered as an electrostatic adsorption [Ma et al., (2003)]. This action was attributed to the effect of chloride ion of the surfactant and of acid solution and chemisorption of these surfactants on C-steel surface. In addition, other factors such as CMC and structure of surfactant might be affecting the inhibition efficiency. The length of the hydrocarbon chain shows that by increasing the length of the hydrophobic parts of the molecule, more inhibition efficiency was obtained. This effect can be attributed to CMC of the investigated surfactant [Menger et al., (2000)].

Table (1): Data of weight loss measurements for carbon steel in 0.5 M HCl solution in the absence and presence of different concentrations of surfactants at 30 °C.

| Comp. | Conc., M | CR (mm y ⁻¹) | θ | IE% |
|--------|--------------------|-----------------------------|----------|-------|
| Blank | ... | 2.68 | 0.000 | 00.00 |
| AOT | 4x10 ⁻⁵ | 2.13 | 0.205 | 20.5 |
| | 8x10 ⁻⁵ | 1.94 | 0.276 | 27.6 |
| | 2x10 ⁻⁴ | 1.27 | 0.26 | 52.6 |
| | 4x10 ⁻⁴ | 1.17 | 0.33 | 56.3 |
| | 6x10 ⁻⁴ | 1.16 | 0.36 | 56.7 |
| | 8x10 ⁻⁴ | 1.08 | 0.597 | 59.7 |
| TX-100 | 4x10 ⁻⁵ | 1.10 | 0.590 | 59.0 |
| | 8x10 ⁻⁵ | 0.82 | 0.694 | 69.4 |
| | 2x10 ⁻⁴ | 0.48 | 0.820 | 82.0 |
| | 4x10 ⁻⁴ | 0.46 | 0.828 | 82.8 |
| | 6x10 ⁻⁴ | 0.36 | 0.866 | 86.6 |
| | 8x10 ⁻⁴ | 0.341 | 0.873 | 87.3 |
| DTAC | 4x10 ⁻⁵ | 0.80 | 0.700 | 70.0 |
| | 8x10 ⁻⁵ | 0.56 | 0.791 | 79.1 |
| | 2x10 ⁻⁴ | 0.39 | 0.854 | 85.4 |
| | 4x10 ⁻⁴ | 0.35 | 0.869 | 86.9 |
| | 6x10 ⁻⁴ | 0.22 | 0.918 | 91.8 |
| | 8x10 ⁻⁴ | 0.19 | 0.929 | 92.9 |

2. Electrochemical measurements

2.1. Potentiodynamic polarization measurements

The potentiodynamic curves of C-steel in 0.5 M HCl in the absence and presence of DTAC is shown in Fig.(2). Similar curves were obtained for other surfactants (not shown). Corrosion parameters for C-steel in 0.5 M HCl without and with the addition of investigated inhibitors are shown in Table(2). It is clear that the selected surfactants act as mixed- type inhibitors i.e., promoting retardation of both anodic dissolution of C-steel and cathodic hydrogen discharge reaction. This may be due to the small shift of E_{corr} (less than 40 mV) due to addition of inhibitors. The effectiveness of organic inhibitors is related to the extent to which they adsorb and cover the metal surface. The adsorption depends on the structure of inhibitors, on the surface charge of the metal, and on the type of the electrolyte. The IE % of the investigated surfactants decreases as follows (Table.2): DTAC > TX-100 > AOT.

The i_{corr} values decrease with increasing inhibitor concentration, while R_p values increase for all inhibitors Table(2). Both cathodic (β_c) and anodic (β_a) Tafel slopes do not change remarkably, which indicates that the mechanism of the corrosion reaction does not change and the corrosion reaction is inhibited by simple adsorption mode [Cao., (2004)]. The irregular trends of β_a and β_c values indicate the involvement of more than one type of species adsorbed on the metal surface. Small changes in potentials can be a result of the competition of the anodic and the cathodic inhibiting reactions, and of the metal surface condition. Generally, the increase of the inhibitor concentration shifts corrosion potential into a less negative direction, what can be explained by a small domination of the anodic reaction inhibition. The results of weight loss measurements confirm the ones obtained by potentiodynamic investigation.

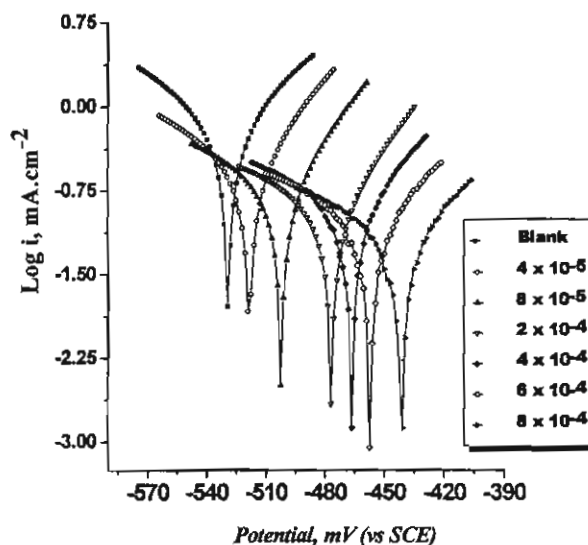


Fig. (2): potentiodynamic polarization for corrosion of C-steel in 0.5 M HCl in the absence and presence of different concentrations of DTAC at 30°C.

Table (2): Potentiodynamic data of carbon steel in 0.5 M HCl and in the presence of different concentrations of surfactants at 30°C.

| Comp. | Conc., M | $-E_{corr}$ vs. SCE, mv | I_{corr} μAcm^{-2} | R_p Ωcm^2 | $-\beta_c$, mV dec^{-1} | β_a , mV dec^{-1} | θ_1 | IE_1 % | θ_R | IE_R % | C.R. $\mu\text{m y}^{-1}$ |
|--------|--------------------|----------------------------------|------------------------------------|------------------------------|--------------------------------------|-------------------------------------|------------|-------------|------------|-------------|------------------------------|
| Blank | 0 | 529 | 516 | 19.9 | 69 | 54 | 0.000 | 00.0 | 0.000 | 00.0 | 5976 |
| AOT | 4×10^{-5} | 528 | 405 | 25.5 | 72 | 51 | 0.215 | 21.5 | 0.219 | 21.9 | 4641 |
| | 8×10^{-5} | 528 | 388 | 26.9 | 72 | 50 | 0.248 | 24.8 | 0.261 | 26.1 | 4495 |
| | 2×10^{-4} | 516 | 284 | 36.2 | 68 | 52 | 0.449 | 44.9 | 0.450 | 45.1 | 2427 |
| | 4×10^{-4} | 515 | 202 | 43.4 | 64 | 46 | 0.608 | 60.8 | 0.541 | 54.1 | 2338 |
| | 6×10^{-4} | 511 | 191 | 48.6 | 67 | 48 | 0.629 | 62.9 | 0.590 | 59.0 | 2212 |
| | 8×10^{-4} | 489 | 182 | 57.8 | 67 | 50 | 0.647 | 64.7 | 0.655 | 65.5 | 2103 |
| TX-100 | 4×10^{-5} | 507 | 225 | 44.58 | 69 | 49 | 0.564 | 56.4 | 0.553 | 55.3 | 2604 |
| | 8×10^{-5} | 496 | 179 | 58.55 | 71 | 51 | 0.653 | 65.3 | 0.660 | 66.0 | 2051 |
| | 2×10^{-4} | 487 | 161 | 64.32 | 70 | 53 | 0.688 | 68.8 | 0.690 | 69.0 | 1860 |
| | 4×10^{-4} | 484 | 140 | 68.64 | 72 | 49 | 0.728 | 72.8 | 0.710 | 71.0 | 1622 |
| | 6×10^{-4} | 483 | 115 | 94.11 | 79 | 52 | 0.777 | 77.7 | 0.788 | 78.8 | 1332 |
| | 8×10^{-4} | 479 | 102 | 97.98 | 81 | 49 | 0.802 | 80.2 | 0.797 | 79.7 | 1179 |
| DTAC | 4×10^{-5} | 518 | 213 | 42.96 | 74 | 41 | 0.587 | 58.7 | 0.536 | 53.6 | 2472 |
| | 8×10^{-5} | 502 | 131 | 69.32 | 77 | 38 | 0.746 | 74.6 | 0.713 | 71.3 | 1517 |
| | 2×10^{-4} | 477 | 87 | 108 | 82 | 39 | 0.831 | 83.1 | 0.815 | 81.5 | 1010 |
| | 4×10^{-4} | 471 | 85 | 111 | 78 | 45 | 0.835 | 83.5 | 0.820 | 82.0 | 993.6 |
| | 6×10^{-4} | 452 | 82 | 120 | 89 | 45 | 0.841 | 84.1 | 0.834 | 83.4 | 954.0 |
| | 8×10^{-4} | 445 | 70 | 137 | 80 | 45 | 0.864 | 86.4 | 0.855 | 85.5 | 809.3 |

2.2. Electrochemical impedance spectroscopy

The EIS provides important mechanistic and kinetic information for an electrochemical system under investigation. Nyquist impedance plots obtained for the C-steel electrode at respective corrosion potentials after 15 min immersion in 0.5 M HCl in the presence and absence of various concentrations of DTAC is shown in Fig.(3). Similar curves were obtained for other inhibitors (not shown). This diagram exhibit a single semi-circle shifted along the real impedance (Z_r) axis. This diagram shows single capacitive loop, which is attributed to charge transfer of the corrosion process, and the diameters of the loops increase with the increase of inhibitor concentration. The R_{ct} values increased with inhibitors concentrations may suggest the formation of a protective layer on the C-steel electrode surface. This layer makes a barrier for mass and charge-transfer. The Nyquist plots (Fig. 3) do not yield perfect semicircles as expected from the theory of EIS, the impedance loops measured are depressed semi-circles with their centers below the real axis, where the kind of phenomenon is known as the "dispersing effect" as a result of frequency dispersion [El Achouri *et al.*, (2001)] and mass transport resistant [K.F. Khaled., (2003)] as well as the heterogeneity of electrode surface resulting from surface roughness, impurities, dislocations, grain boundaries, adsorption of inhibitors, formation of porous layers [Popova *et al.*, (2003), Growcock *et al.*, (1989), Rammet *et al.*, (1987), Mehaute *et al.*, (1983) and Machnikova *et al.*, (2008)]. So, constant phase element (CPE) is substituted for the capacitive element, to explain the depression of the capacitance semi-circle, to give a more accurate fit. Impedance data are analyzed using the circuit in Fig.(4), in which R_s represents the electrolyte resistance, R_{ct} represents the charge-transfer resistance and the constant phase element (CPE). The CPE impedance is obtained by:

$$Z_{CPE} = Y_0^{-1} (j \omega)^{-n} \quad (6)$$

Where: Y_0 is the CPE coefficient, n the CPE exponent (phase shift), ω the angular frequency ($\omega = 2\pi f$, where f is the AC frequency), and j here is the imaginary unit.

When the value of n is 1, the CPE behaves like an ideal double-layer capacitance (C_{dl}) [Machnikova *et al.*, (2008), Gohr *et al.*, (1993), Kliskic *et al.*, (2000) and Babic *et al.*, (2006)]. According to Hsu and Mansfeld, The correction of capacity to its real values is calculated from:

$$C_{dl} = Y_0 (\omega_{max})^{n-1} \quad (7)$$

where ω_{max} is the frequency at which the imaginary part of impedance ($-Z_i$) has a maximum.

The data obtained from fitted spectra are listed in Table(4). The degree of surface coverage (θ) is calculated from the EIS data by using following equation:

$$\theta = \frac{R_{ct} - R_{ct}^*}{R_{ct}} \quad (8)$$

The IE % is calculated from:

$$IE \% = \frac{R_{ct} - R_{ct}^*}{R_{ct}} \times 100 \quad (9)$$

where R_{ct} and R_{ct}^* are the charge-transfer resistances with and without the inhibitors, respectively.

Charge transfer resistance values (R_{ct}) and double layer capacitance values (C_{dl}) were obtained and shown in Table(3). It can be seen from Table(3) that the values of charge transfer resistance increase and the values of C_{dl} decrease, with the inhibitor concentration, which is related to the corrosion inhibition effect of the inhibitor molecules. The decrease in the C_{dl} values which can result from a decrease in local dielectric constant and/or an increase in the thickness of the electrical double layer, suggests that surfactant molecules function by adsorption at the metal/solution interface [Lebrini *et al.*, (2007)].

The inhibition efficiencies, calculated from EIS results, show the same trend as those obtained from polarization measurements. The difference of inhibition efficiency from the two methods may be attributed to the different surface status of the electrode in two measurements. EIS were performed at the rest potential, while in polarization measurements the electrode potential was polarized to high overpotentials, also, due to non-uniform current distributions which resulted from cell geometry, solution conductivity, the position of counter and reference electrodes with respect to working electrode, these will lead to the difference between the two methods [Kelly *et al.*, (2002)].

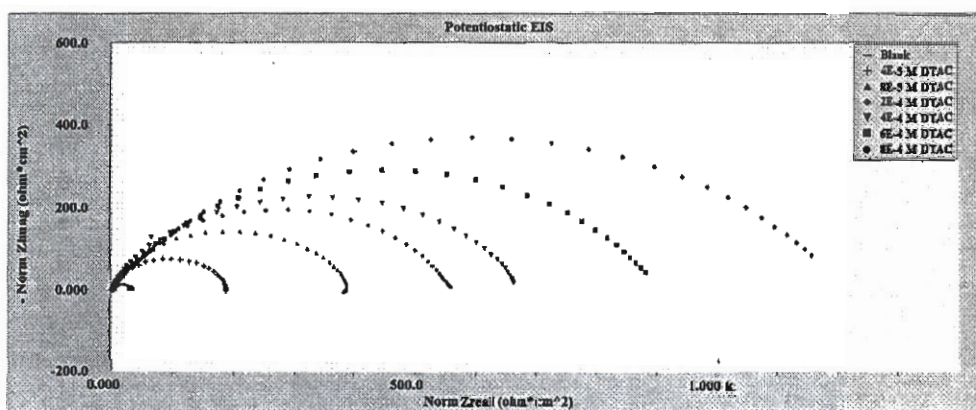


Fig. (3): Nyquist plots for mild steel in 0.5 M HCl in the absence and presence of DTAC.

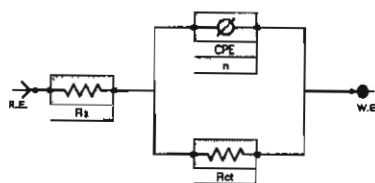


Fig. (4): Equivalent circuit model used to fit the impedance spectra

Table (3): EIS data of carbon steel in 0.5 M HCl and in the presence of different concentrations of surfactants at 30 °C.

| Comp. | Conc., M | R_s (Ωcm^2) | Y ($\mu\Omega^{-1}\text{s}^n$ cm^{-2}) | n | R_{CT} (Ωcm^2) | C_{dl} (μFcm^{-2}) | θ | %IE |
|--------|----------------------|----------------------------------|---|-------|-------------------------------------|--------------------------------------|----------|-------|
| Blank | ... | 1,946 | 0.42,8 | 0.909 | 22,10 | 437 | ... | ... |
| AOT | 4.0×10^{-5} | 2,190 | 281,0 | 0.867 | 47,09 | 236,0 | 0.3183 | 21,82 |
| | 8.0×10^{-5} | 2,074 | 221,8 | 0.886 | 06,42 | 202,6 | 0.4315 | 42,10 |
| | 2.0×10^{-4} | 1,814 | 209,0 | 0.872 | 74,11 | 182,1 | 0.5669 | 06,69 |
| | 4.0×10^{-4} | 2,244 | 160,7 | 0.890 | 84,91 | 120,67 | 0.6220 | 62,20 |
| | 6.0×10^{-4} | 2,284 | 127,8 | 0.889 | 110,0 | 99,22 | 0.7082 | 70,82 |
| | 8.0×10^{-4} | 2,102 | 129,0 | 0.880 | 119,9 | 92,27 | 0.7323 | 72,22 |
| TX-100 | 4.0×10^{-5} | 2,102 | 122,6 | 0.806 | 170,0 | 92,98 | 0.8166 | 81,66 |
| | 8.0×10^{-5} | 1,707 | 78,7 | 0.899 | 110,2 | 08,92 | 0.8312 | 83,12 |
| | 2.0×10^{-4} | 1,830 | 72,6 | 0.897 | 217,9 | 00,46 | 0.8527 | 80,27 |
| | 4.0×10^{-4} | 2,422 | 62,2 | 0.998 | 268,2 | 42,0 | 0.8803 | 88,02 |
| | 6.0×10^{-4} | 1,927 | 09,8 | 0.829 | 202,2 | 28,9 | 0.8941 | 89,41 |
| | 8.0×10^{-4} | 2,006 | 06,1 | 0.846 | 266,8 | 28,7 | 0.8987 | 89,87 |
| DTAC | 4.0×10^{-5} | 1,711 | 112,1 | 0.864 | 187,0 | 79,20 | 0.8288 | 82,88 |
| | 8.0×10^{-5} | 1,830 | 72,48 | 0.849 | 282,0 | 48,87 | 0.9160 | 91,60 |
| | 2.0×10^{-4} | 1,794 | 07,7 | 0.840 | 020,2 | 40,2 | 0.9400 | 94,00 |
| | 4.0×10^{-4} | 1,826 | 00,26 | 0.824 | 227,0 | 27,22 | 0.9496 | 94,96 |
| | 6.0×10^{-4} | 1,726 | 02,20 | 0.907 | 87,0 | 26,22 | 0.9630 | 96,30 |
| | 8.0×10^{-4} | 1,472 | 02,70 | 0.928 | 1120,0 | 26,60 | 0.9717 | 97,17 |

2.3. Electrochemical frequency modulation (EFM)

EFM is a nondestructive corrosion measurement like EIS, it is a small signal ac technique. Unlike EIS, however, two sine waves (at different frequencies) are applied to the cell simultaneously. The great strength of the EFM is the causality factors which serve as an internal check on the validity of the EFM measurement. With the causality factors the experimental EFM data can be verified.

The results of EFM experiments are a spectrum of current response as a function of frequency. The spectrum is called the intermodulation spectrum. The spectra contain current responses assigned for harmonically and intermodulation current peaks. The larger peaks were used to calculate the corrosion current density (i_{corr}), the Tafel slopes

(β_c and β_a) and the causality factors (CF-2 and CF-3). Intermodulation spectra obtained from EFM measurements are presented in Fig.(5) for 0.5 M HCl in absence and presence of 8×10^{-4} M of AOT, TX-100 and DTAC, respectively. Similar curves were obtained for other inhibitors concentration (not shown). As can be seen from Table(4) the corrosion current density decreases by increasing the concentration of the inhibitor. The inhibition efficiency, IE_{EFM} (%) calculated from equation (10) increases by increasing the inhibitor concentration.

$$IE_{EFM} \% = \frac{I_{corr}^0 - I_{corr}}{I_{corr}^0} \times 100 \quad (10)$$

where: I_{corr}^0 and I_{corr} are corrosion current densities in the absence and presence of inhibitors, respectively.

The causality factors in Table(4) are very close to theoretical values which according to the EFM theory [Bosch *et al.*, (2001)] should guarantee the validity of Tafel slopes and corrosion current densities. Here again, the values of i_{corr} recorded by the EFM technique were converted into the corrosion rate (in mmy^{-1}) using equation (4).

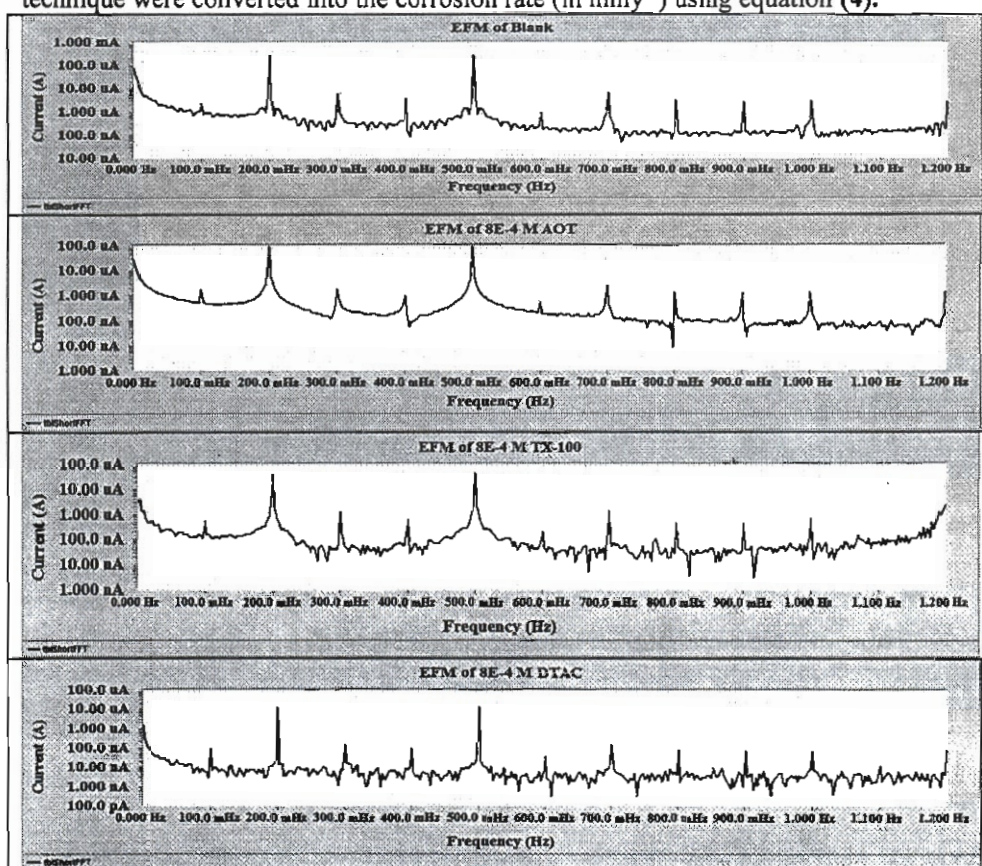


Fig. (5): Intermodulation spectra for C-steel in 0.5M HCl in absence and presence of 8×10^{-4} M concentrations of AOT, TX-100 and DTAC, respectively.

Table (4): Electrochemical kinetic parameters obtained by EFM technique for carbon steel in absence and presence of various concentrations of surfactants in 0.5 M HCl at $30 \pm 1^\circ\text{C}$.

| Comp. | Conc., M | I_{corr} ($\mu\text{A cm}^{-2}$) | β_c (mV dec^{-1}) | β_a (mVdec^{-1}) | CF-2 | CF-3 | CR μm^{-1} | %IE |
|--------|--------------------|--|---------------------------------------|--------------------------------------|------|-------|--------------------------|-------|
| Blank | .,.,. | 488,9 | 127,0 | 1,7,7 | 1,86 | 2,90 | 5763 | .,.,. |
| AOT | 4×10^{-5} | 294,3 | 90,82 | 88,29 | 1,77 | 2,98 | 4575 | 19,24 |
| | 8×10^{-5} | 221,9 | 1,7,9 | 88,22 | 1,84 | 2,92 | 3735 | 24,16 |
| | 2×10^{-4} | 222,8 | 1,2,0 | 87,00 | 1,80 | 2,20 | 3165 | 44,20 |
| | 4×10^{-4} | 228,6 | 91,72 | 87,26 | 1,22 | 2,82 | 2768 | 01,20 |
| | 6×10^{-4} | 208,7 | 97,28 | 87,04 | 1,74 | 2,72 | 2422 | 07,22 |
| | 8×10^{-4} | 117,4 | 94,89 | 82,27 | 1,87 | 2,87 | 1362 | 70,98 |
| TX-100 | 4×10^{-5} | 88,22 | 98,22 | 92,04 | 1,44 | 2,77 | 1020 | 81,92 |
| | 8×10^{-5} | 87,12 | 94,66 | 89,22 | 1,46 | 2,01 | 1011 | 82,18 |
| | 2×10^{-4} | 82,19 | 97,97 | 91,12 | 1,06 | 2,77 | 960 | 82,98 |
| | 4×10^{-4} | 70,00 | 107,2 | 92,84 | 1,72 | 2,64 | 812 | 85,68 |
| | 6×10^{-4} | 07,20 | 98,04 | 84,66 | 1,86 | 2,22 | 602 | 88,46 |
| | 8×10^{-4} | 00,88 | 84,87 | 72,80 | 1,99 | 0,684 | 090 | 89,09 |
| DTAC | 4×10^{-5} | 79,10 | 114,2 | 104,0 | 1,77 | 2,01 | 791 | 82,82 |
| | 8×10^{-5} | 42,46 | 112,8 | 107,2 | 1,00 | 2,12 | 492 | 91,22 |
| | 2×10^{-4} | 41,02 | 121,0 | 112,4 | 1,91 | 2,69 | 476 | 91,61 |
| | 4×10^{-4} | 20,79 | 120,2 | 114,0 | 2,01 | 2,77 | 207 | 92,70 |
| | 6×10^{-4} | 28,77 | 118,2 | 112,6 | 1,72 | 2,67 | 222 | 94,14 |
| | 8×10^{-4} | 27,80 | 149,7 | 124,0 | 1,91 | 2,60 | 222 | 94,20 |

Fig. (6): shows the inhibition efficiency that recorded for DTAC, TX-100 and AOT at a concentration of 8×10^{-4} M using the four different techniques, namely weight loss, Tafel polarization, EIS and EFM. The calculated inhibition efficiencies obtained are in good agreement as shown in Fig.(6).

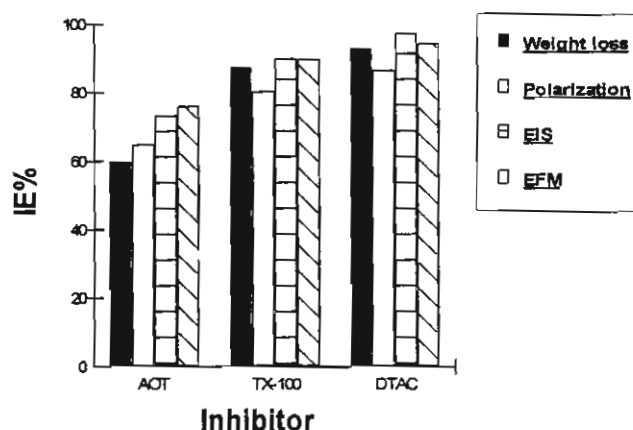


Fig. (6): Comparison of inhibition efficiencies (recorded using EFM, EIS, Tafel polarization and weight loss measurements) obtained for the three surfactants during carbon steel corrosion in 0.5 M HCl solutions containing 8×10^{-4} M of these three surfactants at 30 °C respectively.

2.4. Adsorption of surfactants

The adsorption of ionic surfactants on oppositely charged surface could be taking the following paths [Zhang *et al.*, (2006)]:

1. At low surfactant concentration, the adsorption is due to electrostatic interaction between individual isolated charged monomeric species and the oppositely charged solid surface. Surfactant species begin to form surface aggregates, colloids (surface colloids), including hemi-micelles, admicelles, etc., due to lateral interactions between hydrocarbon chains.
2. When the solid surface is electrically neutralized by the adsorbed surfactant ions, the electrostatic attraction is no longer operative and adsorption takes place due to lateral attraction alone with a reduced slope.
3. When the surfactant concentration reaches critical micelle concentration, the surfactant monomer activity becomes constant and any further increase in concentration contributes only to the micellization in solution and it does not change the adsorption density.

The adsorption in this region is mainly through lateral hydrophobic interaction between the hydrocarbon chains. In steps 2 and 3, surfactant molecules adsorb with a reversed orientation (head groups facing the bulk solution) resulting in a decrease in the hydrophobicity of the particles in this region.

pH plays a very significant role in controlling adsorption of ionic surfactants. Thus the adsorption of anionic surfactants is higher on positively charged surfaces (pH below isoelectric point (IEP)) than on negatively charged surfaces while the cationic surfactants adsorb more on negatively charged surfaces [Koopal *et al.*, (1995) and Fan *et al.*, (1997)]. Molecular structure of surfactant does influence its adsorption behavior markedly.

Most nonionic surfactants contain polar groups that form hydrogen bonds with the hydroxyl groups on the solid surface. Since the hydrogen bonding is weaker than the electrostatic interaction, the adsorption of the nonionic surfactant to most solids is less than that of ionic surfactant. Nonionic surfactants exhibit adsorption similar to those of cationic surfactants, except for a sharp increase in step 3 of the adsorption mechanism because of the absence of electrostatic interactions. The adsorption of the nonionic surfactants also depends on the pH and number of the hydrophilic groups and the hydrocarbon chain length.

Several adsorption isotherms were assessed and the Langmuir adsorption isotherm was found to be the best description of the adsorption behavior of the investigated surfactants in 0.5 M HCl:

$$\frac{C_{inh}}{\theta} = \frac{1}{K} + C_{inh} \quad (11)$$

$$K = \frac{1}{55.5} \exp\left(\frac{-\Delta G_{ads}}{RT}\right) \quad (12)$$

where C_{inh} is the inhibitor concentration, θ is the fraction of the surface coverage, K is the modified adsorption equilibrium constant which can be related to the free energy of adsorption ΔG_{ads} and 55.5 is the concentration of water in mol l^{-1} .

Fig (7) shows the plot of C/θ against C_{inh} for AOT, TX-100 and DTAC give straight lines with almost unit slope, indicating that the tested surfactants obey the Langmuir adsorption isotherm on the C-steel in 0.5 M HCl. The values of ΔG_{ads} recorded in Table 6 are negative, suggesting the spontaneity of the adsorption process. It is well known that values of ΔG_{ads} of the order of 20 kJ mol^{-1} or lower indicate a physisorption, while those of the order of 40 kJ mol^{-1} or higher involve charge sharing or charge transfer from the inhibitor molecules to the metal surface to form a coordinate type of bond [Donahue *et al.*, (1965), Khamis *et al.*, (1991)]. The calculated values of ΔG_{ads} for DTAC are around $-39.8 \text{ kJ mol}^{-1}$, for TX-100 approximately $-39.4 \text{ kJ mol}^{-1}$ and for AOT approximately $-33.5 \text{ kJ mol}^{-1}$, so physisorption and some of chemisorption are purposed.

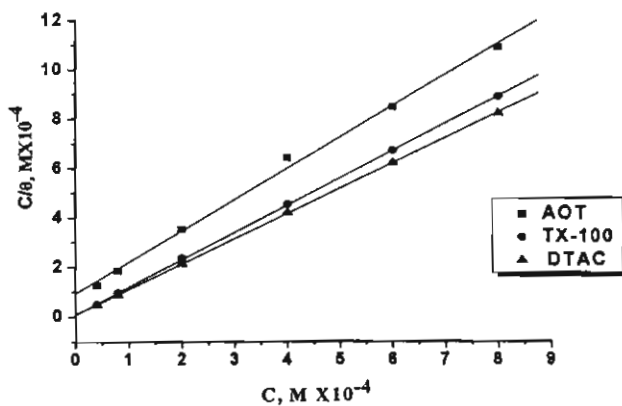


Fig. (7): Langmuir's adsorption plots for C-steel in 0.5M HCl containing various concentrations of surfactants.

Table (6): Values of adsorption isotherms parameters

| Inhibitor | Temp (K) | Adsorption isotherm | $K \times 10^{-4}$ | slope | $-\Delta G_{ads}$ KJ mol ⁻¹ | R ² |
|-----------|----------|---------------------|--------------------|-------|---|----------------|
| AOT | 303 | Langmuir | 1.08 | 1.27 | 33.51 | 0.998 |
| TX-100 | | | 10.95 | 1.10 | 39.36 | 0.999 |
| DTAC | | | 12.92 | 1.02 | 39.77 | 0.999 |

CONCLUSIONS

The main conclusions drawn from this study are:

- The surfactants inhibit the corrosion of C-steel in 0.5 M HCl
- The inhibition is due to adsorption of the inhibitor molecules on the C-steel surface and blocking its active sites.
- Adsorption of the inhibitor fits a Langmuir isotherm model.
- Results obtained from weight loss, dc polarization, ac impedance and EFM techniques are in reasonably good agreement and show increased inhibitor efficiency with increasing inhibitor concentration.
- Polarization data shows that the used surfactants act as mixed-type inhibitor in 0.5 M HCl.

REFERENCES

- Babic-Samardzija, K. and Hackerman, N., *Anti-Corros. Method Mater.* 53 (2006) 19.
- Banerjee G., Malhotra S.N., *Corrosion* 48 (1992)10.
- Bosch R.W., Hubrecht J., Bogaerts W.F. and Syrett B.C., *Corrosion* 57 (2001) 60.
- Cao C.N., *Corrosion Electrochemistry Mechanism*, Chemical Industrial Engineering Press, Beijing, 2004. p. 325 (in Chinese).
- Donahue F.M. , Nobe K. J., *Electrochem. Soc.* 112 (1965) 886.
- El Achouri M., Kertit S., Gouttaya, H.M. , Nciri B., Bensouda Y., Perez L., Infante M.R. and Elkacemi K., *Prog. Org. Coat.* 43 (2001) 267.
- Fan A-X, Somasundaran P, Turro NJ., *Langmuir* 1997;13:506.
- Gohr H., Schaller J. and Schiller C.A., *Electrochim. Acta* 38 (1993) 1961.
- Growcock F.B., Jasinski J.H., *J. Electrochem. Soc.* 136 (1989) 2310.
- Hallen J.M., *Appl. Surf. Sci.* 252 (2006) 2894.
- Kelly R.G., Scully J.R., Shoosmith D.W. and Buchheit R.G., *Electrochemical Techniques in Corrosion Science and Engineering*, Marcel Dekker, Inc., New York, 2002. p. 148.
- Khaled K.F., *Electrochim. Acta* 48 (2003) 2493.
- Khamis E., Belluci F., Latanision R.M. and El-Ashry E.S.H., *Corrosion* 47 (1991) 677.
- Kissi M., Bouklah, M., Hammouti B. and Benkaddour M., *Appl. Surf. Sci.* 252 (2006) 4190.
- Kliskic M., Radosevic J., Gudic S. and Katalinic V. J., *Appl. Electrochem.* 30 (2000) 823.
- Koopal L, Lee E, Böhmer M., *J Colloid Interface Sci* 1995;170:85.
- Lagrenée M., Mernari B., Bouanis M., Traisnel M., and Bentiss F., *Corros. Sci.* 44 (2002) 573.
- Lebrini M., Lagrenée M. , Traisnel M., Gengembre L., Vezin H. and Bentiss F. *Appl. Surf. Sci.* 253 (2007) 9267.

Ma H., Chen S., Yin B., Zhao S. and Liu X., *Corros. Sci.* 45 (2003)867-882.

Machnikova E., Pazderova M., Bazzaoui M., and Hackerman N., *Surf. Coat. Technol.* 202 (2008) 1543.

Mehaute A.H. and Grepy G., *Solid State Ionics* 9-10 (1983) 17.

Menger F.M., and Keiper J.S., *Chem.Int.Ed.*, 39(2000)1906.

Oddo J.E. and Tomson M.B., *J. Pet. Tech* (1982) 1583.

Olivares O., Likhanova N.V. and Gomez B., Navarrete J., Llanos-Serrano M.E., Arce, E. and Hallen J.M., *Appl. Surf. Sci.* 252 (2006) 2894.

Popova A., Sokolova E., Raicheva, S. and Christov M., *Corr. Sci.* 45 (2003) 33.

Rammet U. and Reinhart G., *Corros. Sci.* 27 (1987) 373.

Ridd B., Blakset T.J., and Queen D., *Corrosion, NACE, Paper No (78)*, Houston, Texas, 1998.

Tamil Selvi S., Raman V. and Rajendran, N., *J. Appl. Electrochem.* 33 (2003) 1175.

Zhang R and Somasundaran P., *Advances in Colloid and Interface Science* 123-126 (2006) 215.

المخلص العربي

استخدام بعض المركبات ذات النشاط السطحي لتآكل الصلب الكربوني في المحاليل الحامضية
يحيى عبد اللطيف العواضى - عبد العزيز فودة - حسن كمال عبد العزيز

تم استخدام بعض المركبات ذات النشاط السطحي كمثبطات لتآكل الصلب الكربوني في ٠,٥ مولر حمض الهيدروكلوريك بطرق كيميائية (فقد الوزن) وكهروكيميائية (الاستقطاب البوتنشوديناميكي، المعاوقة الكهروكيميائية و التردد الكهروكيميائي المعدل). وجد من النتائج ان كفاءة التثبيط تعتمد على تركيز هذه المركبات والتركييب الكيميائي لها. وقد دلت طريقة الاستقطاب البوتنشوديناميكي على ان هذه المركبات تعمل كمثبطات مختلطة (انودية و كاثودية) وان ادمصاص هذه المركبات على سطح الصلب الكربوني تتبع ايزوثيرم لانجمير.